HHS Public Access

Author manuscript

Oncogene. Author manuscript; available in PMC 2017 March 30.

Published in final edited form as:

Oncogene. 2008 November 06; 27(52): 6679–6689. doi:10.1038/onc.2008.264.

Overlapping gene expression profiles of cell migration and tumor invasion in human bladder cancer identify metallothionein E1 and nicotinamide N-methyltransferase as novel regulators of cell migration

Y. Wu[1], **M. S. Siadaty**[2], **M.E. Berens**[3], **G. M. Hampton**[4], and **D. Theodorescu**[1]

[1]Department of Molecular Physiology and Biological Physics, University of Virginia Health Sciences Center, Charlottesville, VA

[2]Department of Public Health Sciences, University of Virginia Health Sciences Center, Charlottesville, VA

[3]Cancer and Cell Biology Division, the Translational Genomics Research Institute, Phoenix, AZ

[4]Genomics Institute of the Novartis Research Foundation, San Diego CA

Abstract

Cell migration is essential to cancer invasion and metastasis and is spatially and temporally integrated through transcriptionally dependent and independent mechanisms. Since cell migration is studied in vitro, it is important to identify genes that both drive cell migration and are biologically relevant in promoting invasion and metastasis in patients with cancer. Here, gene expression profiling and a high throughput cell migration system answers this question in human bladder cancer. In vitro migration rates of 40 microarray profiled human bladder cancer cell lines were measured by radial migration assay (RMA). Genes whose expression was either directly or inversely associated with cell migration rate were identified and subsequently evaluated for their association with cancer stage in 61 patients. This analysis identified genes known to be associated with cell invasion such as versican, and novel ones, including metallothionein E1 (MTE1) and nicotinamide N-methyltransferase (NNMT), whose expression correlated positively with cancer cell migration and tumor stage. Using loss of function analysis, we show that MTE1 and NNMT are necessary for cancer cell migration. These studies provide a general approach to identify the clinically relevant genes in cancer cell migration and mechanistically implicate two novel genes in this process in human bladder cancer.

Correspondence to: D. Theodorescu.

Y. Wu Department of Molecular Physiology and Biological Physics, Box 422, University of Virginia Health Sciences Center, Charlottesville, Virginia, 22908. Phone: (434) 924-0042, FAX: (434) 982-3652. yw6s@virginia.edu
D. Theodorescu. Department of Molecular Physiology and Biological Physics, Box 422, University of Virginia Health Sciences Center, Charlottesville, Virginia, 22908. Phone: (434) 924-0042, FAX: (434) 982-3652. dt9d@virginia.edu
M. S. Siadaty: Department of Public Health Sciences, Division of Biostatistics, Box 674, University of Virginia Health Sciences Center, Charlottesville, Virginia, 22908. Phone: (434) 924-8742, FAX: (434) 924-2597. mss4x@virginia.edu
M.E. Berens. The Translational Genomics Research Institute, 445 North 5th Street, Suite 500, Phoenix, AZ 85004. Phone: (602) 343-8760, FAX: (602) 343-8844. mberens@tgen.org
G. M. Hampton, Genomics Institute of the Novartis Research Foundation, 10675 John Jay Hopkins Drive, San Diego, CA, 92121. Phone: (858) 812-1522, FAX: (858) 812-1746. garret_hampton@yahoo.com

Competing interests: The authors declare that they have no competing financial interests.

Keywords

Mechanism of Cell Movement; Metastasis; Gene Expression; Transcriptional Profiling

INTRODUCTION

Cell migration is an integrated multistep process that orchestrates embryonic morphogenesis, tissue repair and regeneration and drives disease progression in many diseases including cancer. Bladder cancer is common in the United States (Jemal *et al.*, 2005) with an estimated 60,000 new cases in 2008. Despite successful treatment of non invasive disease, up to 30% eventually progress to muscle-invasive forms of the disease associated with a 50% mortality rate (Stein *et al.*, 2001).

Recent use of microarray technology has revolutionized our understanding of human cancer including insights into genes involved in tumorigenesis and metastasis (Ramaswamy *et al.*, 2003), the discovery of tumor biomarkers (Dyrskjot *et al.*, 2003; Liotta and Petricoin, 2000), the molecular classification of common neoplasms (Su *et al.*, 2001) and the prediction of drug sensitivity (Lee *et al.*, 2007). For example genes associated with metastasis either positively (metastasis promoter) (Clark *et al.*, 2000) or negatively (metastasis suppressor) (Gildea *et al.*, 2002) has been reported. By analyzing human melanoma cells on DNA microarrays, high expression of RhoC was identified to correlate with the metastatic phenotype. In animal experiments, RhoC enhanced metastasis when overexpressed, whereas its dominant-negative Rho inhibited metastasis (Clark *et al.*, 2000). Others have shown that RhoC plays a critical role in tumour cell migration (Faried *et al.*, 2006; Mukai *et al.*, 2006). Together, this data indicates that RhoC plays a role in both in vivo metastasis and cell migration. Similar tools were used to identify RhoGDI2 as a metastasis suppressor gene and inhibitor of EGF stimulated tumor cell migration (Gildea *et al.*, 2002; Theodorescu *et al.*, 2004; Titus *et al.*, 2005).

Given this demonstrated utility, use of this technology to identify key genes involved in cell migration appears feasible. In addition, identifying a subset of such genes that are also associated with cancer progression in patients would provide assurance of their biological relevance in human disease. Here we use genome wide expression profiling to define a “gene expression signature” of bladder cancer cell migration. We further evaluate the dependency of these signatures on different extracellular matrices upon which the cells are plated. With the goal of focusing only on those transcriptional networks that are relevant to human bladder cancer invasion, we further refine this migration signature with input of gene expression profiles derived from human cancer tissues and select only those genes which correlate with both cell migration and tumor stage. Once identified, we evaluate the mechanistic significance of these findings on cell migration using siRNA mediated mRNA depletion. Gene products causally related to cell migration are targets for anti-invasive therapies and candidate biomarkers for progression in patients.

RESULTS

The type of extracellular matrix affects in vitro bladder cancer cell migration

The radial migration assay was used to measure migration of bladder cancer cell lines. The average migration speeds of 40 human bladder cancer cells on different matrices were computed and summarized (Table 1). The regression model was used to classify bladder cancer cell lines into 2 groups of cell lines: Group 1: rapidly migrating cells and Group 2: slow migrating cells as defined in materials and methods (Table 1). Examination of rates of cell migration indicates a large baseline (i.e. glass) variation among the cell lines (Figure 1B). In addition, cells plated on fibronectin, laminin and collagen have enhanced cell migration compared to those cells grown on BSA, or glass, ($p<0.05$) (Figure 1C). Furthermore, among the 3 matrices, cells appear to move the fastest on collagen type 4 ($p<0.01$). Differences in baseline (intrinsic) migration speeds among the cell lines explain ~70% of the total variation observed, versus 4% explained by the matrix types (with both cell lines and matrix types being statistically significant terms in the model, $p<0.001$). Interestingly, cells with higher rates of migration on glass tend to be less sensitive to the effects of matrix for their migration (Figure 1D).

Gene expression profiling of cancer cell migration and its relation cell matrix

Oligonucleotide microarray profiling of the bladder cancer cell lines was used to determine the commonality and differences between expression profiles associated with cell migration on different matrices. To accomplish these goals we compared the gene expression profiles of cell line groups with fast or slow migration speeds on different matrices. With the criteria of expression fold changes ≥ 3 and statistical significance p-value ≤ 0.01, we determined that 236 gene probes were associated with migration rate on either control (glass) or specific matrices (supplementary Table 1). A Venn diagram was used to classify the numbers of gene probes associated with migration rate on one or a combination of different matrices. 49 gene probes are commonly associated with migration rate on all five surfaces, while 3, 11 and 43 probes specifically depend on laminin, fibronectin and collagen IV matrices, respectively while 4 are specific to glass (Figure 2A and supplementary Table 1).

Results of Ingenuity® pathway analysis with probes either associated with migration on specific surfaces or all substrates are shown in Table 2. When the 49 probes which were associated with migration rate on all five surfaces were examined, only one pathway, O-glycan Biosynthesis was found significant. In contrast, when the analysis was carried out on the probe sets that were associated with migration on specific surfaces, different pathways emerged. O-glycan Biosynthesis, Integrin signaling, eicosanoid signaling and Wnt/β-Catenin Signaling were the only significant pathways and given the multitude of pathways available, suggests that bladder cancer has a relatively restricted set of biochemical signaling pathways upon which migratory behaviors are dependent.

Versican, NNMT and MT1E expression are associated with cell migration and tumor stages

To select clinically relevant genes associated with cell migration, we evaluated the expression profiles of the genes discovered in the cell line migration assay as a function of tumor stage in human bladder cancer. We reasoned that a gene whose expression correlates

with speed of migration in vitro is important for in vivo cancer invasion if such expression also correlates with tumor stage in human cancer. Microarray data from 15 normal urothelia, 25 superficial (Ta) and 21 invasive tumors of stage T2 and above was evaluated to determine which migration genes (Figure 2A) were associated with malignancy (normal vs. tumor) and progression (superficial vs. invasive tumor) (supplementary Table 1). The rationale for carrying out both of these comparisons was that some genes may be important in conferring enhanced cell migration to cells upon transformation while others enhance this phenotype during tumor progression. The differentially expressed gene probes associated with both cell migration and tumor stages are shown in Table 3. The elevated expression of versican (chondroitin sulfate proteoglycan 2) is shown to correlate not only to three types of matrix-dependent cell migration, but also tumor transformation and progression.

Four genes, nicotinamide N-methyltransferase (NNMT), putative secreted protein XAG, ephrin-B2 and mesoderm specific transcript homolog (MEST) were associated with fibronectin and collagen IV dependent cell migration while also associated with tumor stage. Thirteen individual gene probes were involved in one matrix dependent cell migration while also implicated in tumor transformation or progression. In the case of the glass or BSA coated surface, metallothionein 1E (MT1E) and three other genes were found to associate with higher expression in fast migrating cell lines and transformation or progression in human tumor tissues. Evaluation of the literature also indicated that NNMT and MT1E expression is strongly associated with tumor stage in two other large studies in bladder cancer (Figure 2B). Furthermore, examination of the NNMT and MT1E expression levels across the 40 cell lines used in the study reveals no correlation between them (Figure 2C) suggesting these levels are regulated by different factors and that these genes are likely members of distinct pathways regulating to tumor progression. Taken together, given the novel association of NNMT and MT1E with tumor invasion and in vitro migration, these genes were selected for further study to determine if they have a mechanistic role in cell migration in vitro and in vivo.

Depletion of NNMT affects chemotaxis and chemokinesis

To investigate whether chemotaxis is regulated by NNMT we chose 253J laval human bladder cancer cells which have high NNMT expression. These cells migrate well toward 2% FBS media in the transwell migration chamber assay. We transiently transfected 253J laval cells with two NNMT-specific siRNA oligonucleotides NNMT-A and NNMT-B, and in view of the absence of commercially available or academic source of antibody, real-time RT-PCR analysis was used to confirm reduction of NNMT mRNA level for both NNMT-specific siRNA oligonucleotides (Figure 3A). The decrease of NNMT expression ranged from 86% to 90%, compared with non-specific luciferase knockdown. Importantly, both knockdowns of NNMT resulted in a significant decrease of chemotaxis responses to 2% serum media, compared with non-specific luciferase knockdown (Figure. 3B). To evaluate the role of NNMT in bladder cancer chemokinesis, we tracked the movement of individual cells using time-lapse microscopy. Tracked movements from all cells in randomly-selected fields of view were plotted (Figure 3C). The average distance traveled by cells from NNMT or luciferase knockdown was quantified (Figure 3D). In 3 hours, the average migration distance

(11.3±6.3 um) of 21 cells with NNMT knockdown was considerably shorter than that (17.9±6.4 um) from 27 cells without NNMT depletion ($p< 0.001$).

Knockdown of MT1E decreases cell migration in the wound healing assay

A similar experiment to that for NNMT was carried out to test whether reduction of endogenous MT1E expression would affect serum chemotaxis in SLT4 human bladder cancer cells, which have high expression of MT1E. Despite successful knockdown of MT1E mRNA (no commercially available or academic source of antibody), no effect on transwell migration was seen (data not shown). Similarly, knockdown of MT1E in SLT4 cells did not affect chemokinesis (data not shown). We thus evaluated cell migration in the wound healing assay in response to depletion of MT1E and NNMT. SLT4 cells were transfected with siRNA's to pGL2 as well as either of two oligos to MT1E (MT1E-A and MT1E-B). 48 hours after transfection, real-time RT-PCR analysis was used to evaluate reduction of MT1E mRNA level (Figure 4A). In parallel replica plates, we analyzed migration of cultured SLT4 cells in wound assays for an additional 12 hours. Comparison between starting wounds and wounds at 12 hours, indicated that MT1E-A and MT1E-B depletion results in decreased of wound healing of SLT4 cells (Figure 4B,C).

Knockdown of NNMT or MT1E causes decreased cell proliferation

To evaluate the impact of NNMT or MT1E depletion on growth, 5×10^3 SLT4 or 253J laval cells were plated in each well of 24-well plates and siRNA transfection carried out. Real-time PCR analysis was used to confirm reduction of NNMT and MT1E mRNA level and measurement of cell number evaluated over 4 days. As seen in Figure 5A, cell proliferation in 253J laval depleted of NNMT by both siRNA oligos was reduced compared to pGL2 knockdown control. At day 4 after the siRNA transfection, NNMT-A siRNA oligonucleotide decreased cell number by 24% ($p=0.048$) from luciferase controls, while NNMT-B oligonucleotide caused a decrease of cell number by 40% ($p=0.019$). MT1E siRNA knockdown in SLT4 cells also led to decreased cell proliferation in two independent experiments. In general, MT1E-A and MT1E-B siRNA oligonucleotides decreased SLT4 cell numbers by 21–25% four days after the siRNA oligonucleotide transfections for both MT1E-A and MT1E-B (Figure 5B). Stable depletion of both genes was attempted using shRNA but no cells with depleted levels were obtained (data not shown). We suspect, given the decreased proliferation, such cells would have been overgrown by cells without significant depletion of the genes, resulting in the observed phenotype.

DISCUSSION

Bladder cancer can present either as a non-invasive or invasive lesion with up to 30% of the former progressing to invasiveness over time (Witjes, 2006). Recently, gene expression profiles depicting bladder cancer progression have been assembled (Dyrskjot *et al.*, 2003; Modlich *et al.*, 2004; Sanchez-Carbayo *et al.*, 2003; Thykjaer *et al.*, 2001). To the extent that in vitro cancer cell migration approximates some of the processes of in vivo tumor invasion, a better understanding of the gene expression changes associated with migration may assist in screening approaches to identify genes that underlie malignant invasion as well as supporting the discovery of drugs to control cancer invasion and metastasis. Here we report

an initial step towards developing a molecular connection between in vitro migration and in vivo invasion. We anticipate that this will mature into a method to identify genes associated with cell migration that are also likely candidates involved in tumor invasion in patients with bladder cancer. Extension of this approach to other tumor types is also feasible.

In the present report, we use bladder cancer as a model system to examine migration of 40 cancer cell lines on different extracellular matrices found in vivo and relate data from their gene expression profiling to migratory rate. Importantly, this work does not assume or depend on whether gene expression on plastic is representative of gene expression on the different matrices but uses these as reference for anchoring the migration phenotypes on different strata. Interestingly, differences in migration speeds among the cell lines are determined by both cell line and by matrix type with the largest contribution attributable to inherent features of the cell line. A dependency of migration on matrix type in bladder cancer cells has been also shown by others. For example, EJ cells (T24T), when grown on extracellular matrix (ECM) derived from ras transfected fibroblast cells, have a higher growth and motility rate than when grown on ECM derived from normal fibroblasts (Gordon *et al.*, 1993). The increased cell migration results from up-regulation of type IV collagen mRNA expression in EJ cells grown on ECM derived from ras transfected fibroblasts. In our radial migration assay, collagen IV also considerably promotes cell migration of EJ (T24T) cell line.

Computational pathway analysis of gene probes associated with matrix dependent cell migration on a relatively large scale for one tissue type can complement detailed work on individual cell lines. For example, our studies demonstrated that fibronectin-dependent migration of bladder cancer cells is associated with the ecosanoid and Wnt/β-Catenin signaling pathways while fibronectin was reported to stimulate the motility of invasive human bladder cancer T24 cells via PKC signal transduction pathways (Margolis *et al.*, 1996). By virtue of using 40 cell lines and querying which genes associate with migration on all surfaces, this approach may identify gene products and signaling pathways that are generally relevant in human bladder cancer rather than being limited to specific matrix models. This notion is supported by finding that O-glycan Biosynthesis is the only pathway statistically correlated with the 49 probes associated with migration rate on all five surfaces. Interestingly, mucin-type glycoproteins carrying sialylated, fucosylated glycans are known to be metastasis-associated biomarkers (Altevogt *et al.*, 1988; Kristiansen *et al.*, 2004). In fact, we have recently shown that one such molecule, CD24, a ligand for P-selectin (Aigner *et al.*, 1997; Friederichs *et al.*, 2000), is both a biomarker for bladder cancer progression (Smith *et al.*, 2006) as well as necessary for bladder cancer growth (Smith *et al.*, 2006) in vitro. Furthermore, CD24 is a biomarker for metastasis in many common human cancers (Smith *et al.*, 2006).

Among our identified candidate migration/progression genes, versican, ephrin-B2 and E-cadherin are well known to be associated with tumor transformation and progression. We also identified E-cadherin and fibronectin 1 as biomarkers for both cell migration and tumor stage consistent with data from other microarrays (Modlich *et al.*, 2004; Thykjaer *et al.*, 2001). Elevated levels of extracellular matrix versican are also predictive of poor prognosis in patients with prostate cancer, endometrial cancer and oral squamous cell carcinoma

(Kodama *et al.*, 2006; Pukkila *et al.*, 2006; Ricciardelli *et al.*, 1999). The G3 isoform of versican directly binds to fibronectin, complexing with VEGF, and enhances colony growth in soft agar and tumor growth and blood vessel formation in nude mice (Zheng *et al.*, 2004).

Our study is the first to identify N-methyltransferase (NNMT) and metallothionein (MT) 1E as contributors to bladder cancer migration in vitro while being associated with human tumor invasion in patients. NNMT has been identified as a novel serum marker for human colorectal cancers (Roessler *et al.*, 2005) despite the fact that this protein is not predicted to be secreted but is considered to be restricted to the cytoplasmic compartment. Other authors report overexpression of NNMT in papillary thyroid cancer, renal carcinoma and gastric cancer (Lim *et al.*, 2006; Roessler *et al.*, 2005; Xu *et al.*, 2003; Yao *et al.*, 2005). It is also interesting to note that NNMT works in a xenobiotic pathway to maintain homeostasis (Aksoy *et al.*, 1995; Aksoy *et al.*, 1994) while metallothioneins (MTs) are small, cysteine-rich zinc binding proteins that are powerful antioxidants. In eight out of ten prediction models of toxicogenomics, MT1E is predicted to be involved in carcinogenic process (van Delft *et al.*, 2005) and MT1E is predicted to be a biomarker in hepatocellular carcinoma (Grate, 2005). Interestingly, the antioxidant Genistein can up-regulate transcription of MT1E (Chung *et al.*, 2006). In addition to their roles in bladder cancer migration, depletion of NNMT and MT1E are also associated with decreased cell proliferation, making these proteins even more interesting targets for therapy. Interestingly, MT protein was also shown to be elevated in estrogen-receptor-negative breast cancer cell lines that express MT-1E mRNA suggesting a possible relationship between estrogen receptor status and MT-1E gene expression in human breast cancer (Friedline *et al.*, 1998; Jin *et al.*, 2000).

These data are also interesting since bladder cancer is regarded as a chemical carcinogenesis disease (Jones *et al.*, 1992) and the present work is the first to link genes involved with detoxification to the migratory/invasive process. Hinting at such a relationship is the finding that chemical carcinogen derived murine bladder cancers are most likely to be invasive, and their gene expression profile is more closely related to that of invasive bladder cancer than noninvasive bladder cancer (Williams and Theodorescu, manuscript in preparation). Hence, further study of NNMT and MT1E may discover new links between chemical carcinogenesis and tumor progression in bladder cancer.

MATERIALS AND METHODS

Radial Migration Assay (RMA)

Migration assays were performed using a 96-well monolayer radial migration assay (Berens and Beaudry, 2004). Wells were either left uncoated or coated with 0.1% BSA, 10μg/ml laminin, 10μg/ml fibronectin or 10μg/ml collagen type IV in PBS for 1 hour at 37°C, rinsed three times in PBS, and then blocked with 0.1% BSA in PBS for 30 minutes at room temperature. Bladder cancer cell lines were plated at 3,000 cells/well and incubated for 6 hours to allow attachment. After attachment, the diameter of each cell population was measured (time 0) using an inverted microscope and image analysis software (Scion Image Corp, Frederick, MD) (Figure 1A). Cells were incubated for an additional 24 hours and second diameter measurements were taken. *Migration speed* is reported as the specific radial movement D2-D1 (μm/day) of the cell population. The migration assays were done in six

replicates for each condition and were then carried out similarly in a repeat experiment one week later.

Transwell, Time-lapse and Wound Migration Assays

253J Laval and SLT4 cell lines (Nicholson *et al.*, 2004; Titus *et al.*, 2005) were maintained as described. 48 hours after siRNA transfection, cells were harvested, counted and resuspended in serum-free media. 5000 cells of 253J Laval or 10,000 cells of SLT4 were added in triplicate to the upper chambers of transwell filters (8.0 um pores, Becton Dickinson, Franklin Lakes, NJ) in 24 well tissue culture plates and the assay carried out as described (Oxford *et al.*, 2005). For time lapse microscopy cells were prepared as for the transwell assay and assay carried out as described (de Rooij *et al.*, 2005) with images captured every 2.5 minutes for 3 hours on a temperature controlled stage of a Nikon TE200 inverted microscope. For the wound healing assay, cells were seeded in 6 well plate and transfected with NNMT or MT1E siRNA oligonucleotides for 48 hours. Midline wounds were inflicted by a plastic pipette tip. Immediately after scratching and again after 12 hours, well images were evaluated and analyzed as described (Gildea *et al.*, 2002).

Transcriptional Profiling of Bladder Tumor Cell Lines and Human Bladder Cancers

Human bladder-carcinoma derived cell lines, primary human bladder carcinoma tissues and normal bladder urothelium were profiled on HG-U133A GeneChip arrays (Affymetrix, Santa Clara, CA, USA) as described (Titus *et al.*, 2005). Further datasets of primary bladder cancer samples obtained from tumors of known pathological stages and grades as well as samples of normal urothelium were obtained from the literature (Smith *et al.*, 2007). Image files were assessed for quality and artifacts and processed using Microarray Analysis Suite 5.0 (MAS 5.0, Affymetrix, Santa Clara, CA, USA) using a scaling factor of 200.

Statistical Analysis of Human Bladder Cancer Cell Migration

For each matrix type, we fitted a regression model where migration speed is the dependent variable, while cell line type is the independent variable (Team, 2003). We used a ‘deviation’ contrast for the categorical variable representing the cell lines. Hence, the model estimates an overall average migration speed, and then compares speed of each cell line to it. This gives us a group of cell lines with migration speeds significantly higher than average (defined as rapid migrating cells), a group where speeds are significantly lower than average (defined as slow migrating cells), and a third group of insignificant speed difference from average. This method is suited to the situation where no external criterion is available for defining cutoffs for fast and slow speeds. Another advantage of this method is to eliminate noise introduced by borderline cell lines. Disadvantages include decreased sample size. The Student’s t-test was used to determine significant differences in comparisons between two groups. Two-tailed distribution and two-sample unequal variance were used to make comparisons.

Identification and Network Analysis of Genes Associated with Cell Migration Speed and Tumor Stage

We used the Bioconductor LPE library for analysis of gene expression (www.bioconductor.org). To discover differentially expressed genes, we computed the false discovery rate (FDR), and used the BH option for multiple comparison adjustments. We used two criteria to select genes: 1) fold change ≥ 3, and 2) statistical significance ≤ 0.01. We applied the above analysis and two criteria to two separate datasets: 1) gene expression of the cell migration experiment, and 2) gene expression associated with clinical stage of tumors. For the migration expression data, we located genes up- and down-regulated in slow versus fast groups defined as above within each matrix type. For the stage expression data we located genes up- and down-regulated in noninvasive (stage Ta and normal) versus invasive (stage ≥T2) tumors. Then we selected genes that are: 1) overexpressed in fast migration group and in the invasive tumors; 2) genes that are overexpressed in the slow migration group and in non invasive cancers. Among such genes, we identified genes that are common in all the matrix types, versus ones that are specific to different types of matrices. To identify networks associated with cell migration, the data was explored with Ingenuity Systems pathways analysis software (www.ingenuity.com) as previously described (Calvano *et al.*, 2005; Li *et al.*, 2006; Mayburd *et al.*, 2006).

siRNA Mediated mRNA Depletion

siRNA oligonucleotides (final concentration 100nM) transfection was conducted using Oligofectamine (Invitrogen, CA). The luciferase pGL2, two NNMT-specific siRNA oligonucleotides NNMT-A: GAAAGAGGCTGGCTACACA and NNMT-B: GAGGTGATCTCGCAAAGTT, two MT1E-specific siRNA oligonucleotides MT1E-A: ATAGAGCAGCCAGTTGCAG and MT1E-B: TGACTGCTTGTTCGTCTCA, were ordered from Dharmacon (Lafayette, CO). At 48 hours after the transfections, cells were subjected to RNA extraction using a RNeasy mini kit. RNA was reverse transcribed using the random primers of the ImPrompII kit (Promega, WI). The real-time PCR assay was conducted in iCycler IQ^{TM} real-time PCR Detection System following the manufacturer's procedures (BioRad, CA). The fluorescent dye IQ^{TM} SYBR Green Supermix was used in PCR reaction (BioRad, CA). The sequences of the real time PCR primers are as follows (5′ to 3′): NNMT-f1055: CCTTTGACTGGTCCCCAGTG, NNMT-r1155: CTGCTTGACCGCCTGTCTC; MT-IE-f102: GGCTCCATTCTGCTTTCCAA, MT-IE-r206: AGTGGCGCAAGAGCAGTTG; β-actin-f-RT, CCAGATCATGTTTGAGACCTTCAAC, and β-actin-r-RT: CCAGAGGCGTACAGGGATAGC.

Cell proliferation assay

5×10^3 SLT4 or 253J Laval cells were incubated in each well of 24-well plates for siRNA transfection and evaluation of cell number. Alamar Blue was diluted 1 to 20 in the cell culture media, and fluorescence emission assessed at 4 hr after addition according to manufacturer protocol (Biosource, CA), on the designated days from siRNA transfection. Colorimetric evaluation was performed using a SPECTRA max spectrophotometer

(Molecular Devices, CA) with 540 nm as excitation wavelength and 590 nm as emission wavelength as described (Havaleshko *et al.*, 2007).

Supplementary Material

Refer to Web version on PubMed Central for supplementary material.

Acknowledgments

The authors thank Drs. Jay Fox and Yongde Bao of the University of Virginia Array Core facility for their assistance with chip hybridization. The authors thank Drs. Martin A Schwartz and Konstadinos Moissoglu of the Cardiovascular Research Center, University of Virginia for their assistance with time-lapse microscopy. Mr. Christian Beaudry at TGen performed the high-throughput cell migration experiments. This work was supported by NIH grant CA075115 to DT.

References

Aigner S, Sthoeger ZM, Fogel M, Weber E, Zarn J, Ruppert M, et al. CD24, a mucin-type glycoprotein, is a ligand for P-selectin on human tumor cells. Blood. 1997; 89:3385–3395. [PubMed: 9129046]

Aksoy S, Brandriff BF, Ward A, Little PF, Weinshilboum RM. Human nicotinamide N-methyltransferase gene: molecular cloning, structural characterization and chromosomal localization. Genomics. 1995; 29:555–561. [PubMed: 8575745]

Aksoy S, Szumlanski CL, Weinshilboum RM. Human liver nicotinamide N-methyltransferase. cDNA cloning, expression, and biochemical characterization. J Biol Chem. 1994; 269:14835–14840. [PubMed: 8182091]

Altevogt P, Lang E, Heckl-Ostreicher B, Benke R, Kratzin H, Schirrmacher V. Changes in metastasis formation and distinct cell surface molecules in adhesion variants of a metastatic murine tumor. Adv Exp Med Biol. 1988; 233:253–258. [PubMed: 2975914]

Berens ME, Beaudry C. Radial monolayer cell migration assay. Methods Mol Med. 2004; 88:219–224. [PubMed: 14634232]

Blaveri E, Simko JP, Korkola JE, Brewer JL, Baehner F, Mehta K, et al. Bladder cancer outcome and subtype classification by gene expression. Clin Cancer Res. 2005; 11:4044–4055. [PubMed: 15930339]

Calvano SE, Xiao W, Richards DR, Felciano RM, Baker HV, Cho RJ, et al. A network-based analysis of systemic inflammation in humans. Nature. 2005; 437:1032–1037. [PubMed: 16136080]

Chung MJ, Kang AY, Lee KM, Oh E, Jun HJ, Kim SY, et al. Water-soluble genistin glycoside isoflavones up-regulate antioxidant metallothionein expression and scavenge free radicals. J Agric Food Chem. 2006; 54:3819–3826. [PubMed: 16719502]

Clark EA, Golub TR, Lander ES, Hynes RO. Genomic analysis of metastasis reveals an essential role for RhoC. Nature. 2000; 406:532–535. [PubMed: 10952316]

de Rooij J, Kerstens A, Danuser G, Schwartz MA, Waterman-Storer CM. Integrin-dependent actomyosin contraction regulates epithelial cell scattering. J Cell Biol. 2005; 171:153–164. [PubMed: 16216928]

Dyrskjot L, Thykjaer T, Kruhoffer M, Jensen JL, Marcussen N, Hamilton-Dutoit S, et al. Identifying distinct classes of bladder carcinoma using microarrays. Nat Genet. 2003; 33:90–96. [PubMed: 12469123]

Faried A, Faried LS, Kimura H, Nakajima M, Sohda M, Miyazaki T, et al. RhoA and RhoC proteins promote both cell proliferation and cell invasion of human oesophageal squamous cell carcinoma cell lines in vitro and in vivo. Eur J Cancer. 2006; 42:1455–1465. [PubMed: 16750623]

Friederichs J, Zeller Y, Hafezi-Moghadam A, Grone HJ, Ley K, Altevogt P. The CD24/P-selectin binding pathway initiates lung arrest of human A125 adenocarcinoma cells. Cancer Res. 2000; 60:6714–6722. [PubMed: 11118057]

Friedline JA, Garrett SH, Somji S, Todd JH, Sens DA. Differential expression of the MT-1E gene in estrogen-receptor-positive and -negative human breast cancer cell lines. Am J Pathol. 1998; 152:23–27. [PubMed: 9422519]

Gildea JJ, Seraj MJ, Oxford G, Harding MA, Hampton GM, Moskaluk CA, et al. RhoGDI2 is an invasion and metastasis suppressor gene in human cancer. Cancer Res. 2002; 62:6418–6423. [PubMed: 12438227]

Gordon JN, Shu WP, Schlussel RN, Droller MJ, Liu BC. Altered extracellular matrices influence cellular processes and nuclear matrix organizations of overlying human bladder urothelial cells. Cancer Res. 1993; 53:4971–4977. [PubMed: 8402687]

Grate LR. Many accurate small-discriminatory feature subsets exist in microarray transcript data: biomarker discovery. BMC Bioinformatics. 2005; 6:97. [PubMed: 15826317]

Havaleshko DM, Cho H, Conaway M, Owens CR, Hampton G, Lee JK, et al. Prediction of drug combination chemosensitivity in human bladder cancer. Mol Cancer Ther. 2007; 6:578–586. [PubMed: 17308055]

Jemal A, Murray T, Ward E, Samuels A, Tiwari RC, Ghafoor A, et al. Cancer statistics, 2005. CA Cancer J Clin. 2005; 55:10–30. [PubMed: 15661684]

Jin R, Bay BH, Chow VT, Tan PH, Lin VC. Metallothionein 1E mRNA is highly expressed in oestrogen receptor-negative human invasive ductal breast cancer. Br J Cancer. 2000; 83:319–323. [PubMed: 10917545]

Jones RF, Debiec-Rychter M, Wang CY. Chemical carcinogenesis of the urinary bladder--a status report. J Cancer Res Clin Oncol. 1992; 118:411–419. [PubMed: 1618888]

Kodama J, Hasengaowa Kusumoto T, Seki N, Matsuo T, Ojima Y, et al. Prognostic significance of stromal versican expression in human endometrial cancer. Ann Oncol. 2006

Kristiansen G, Sammar M, Altevogt P. Tumour biological aspects of CD24, a mucin-like adhesion molecule. J Mol Histol. 2004; 35:255–262. [PubMed: 15339045]

Lee JK, Havaleshko DM, Cho H, Weinstein JN, Kaldjian EP, Karpovich J, et al. A strategy for predicting the chemosensitivity of human cancers and its application to drug discovery. Proc Natl Acad Sci USA. 2007; 104:13086–13091. [PubMed: 17666531]

Li CJ, Li RW, Wang YH, Elsasser TH. Pathway analysis identifies perturbation of genetic networks induced by butyrate in a bovine kidney epithelial cell line. Funct Integr Genomics. 2006

Lim BH, Cho BI, Kim YN, Kim JW, Park ST, Lee CW. Overexpression of nicotinamide N-methyltransferase in gastric cancer tissues and its potential post-translational modification. Exp Mol Med. 2006; 38:455–465. [PubMed: 17079861]

Liotta L, Petricoin E. Molecular profiling of human cancer. Nat Rev Genet. 2000; 1:48–56. [PubMed: 11262874]

Margolis EJ, Choi JC, Shu WP, Liu BC. Specific sequences of fibronectin activate the protein kinase C signal transduction pathway in invasive bladder cancer. Cancer Lett. 1996; 100:163–168. [PubMed: 8620437]

Mayburd AL, Martlinez A, Sackett D, Liu H, Shih J, Tauler J, et al. Ingenuity network-assisted transcription profiling: Identification of a new pharmacologic mechanism for MK886. Clin Cancer Res. 2006; 12:1820–1827. [PubMed: 16551867]

Modlich O, Prisack HB, Pitschke G, Ramp U, Ackermann R, Bojar H, et al. Identifying superficial, muscle-invasive, and metastasizing transitional cell carcinoma of the bladder: use of cDNA array analysis of gene expression profiles. Clin Cancer Res. 2004; 10:3410–3421. [PubMed: 15161696]

Mukai M, Endo H, Iwasaki T, Tatsuta M, Togawa A, Nakamura H, et al. RhoC is essential for TGF-beta1-induced invasive capacity of rat ascites hepatoma cells. Biochem Biophys Res Commun. 2006; 346:74–82. [PubMed: 16750170]

Nicholson BE, Frierson HF, Conaway MR, Seraj JM, Harding MA, Hampton GM, et al. Profiling the evolution of human metastatic bladder cancer. Cancer Res. 2004; 64:7813–7821. [PubMed: 15520187]

Oxford G, Owens CR, Titus BJ, Foreman TL, Herlevsen MC, Smith SC, et al. RalA and RalB: antagonistic relatives in cancer cell migration. Cancer Res. 2005; 65:7111–7120. [PubMed: 16103060]

Pukkila M, Kosunen A, Ropponen K, Virtaniemi J, Kellokoski J, Kumpulainen E, et al. High stromal versican expression predicts unfavourable outcome in oral squamous cell carcinoma. J Clin Pathol. 2006

Ramaswamy S, Ross KN, Lander ES, Golub TR. A molecular signature of metastasis in primary solid tumors. Nat Genet. 2003; 33:49–54. [PubMed: 12469122]

Ricciardelli C, Quinn DI, Raymond WA, McCaul K, Sutherland PD, Stricker PD, et al. Elevated levels of peritumoral chondroitin sulfate are predictive of poor prognosis in patients treated by radical prostatectomy for early-stage prostate cancer. Cancer Res. 1999; 59:2324–2328. [PubMed: 10344737]

Roessler M, Rollinger W, Palme S, Hagmann ML, Berndt P, Engel AM, et al. Identification of nicotinamide N-methyltransferase as a novel serum tumor marker for colorectal cancer. Clin Cancer Res. 2005; 11:6550–6557. [PubMed: 16166432]

Sanchez-Carbayo M, Socci ND, Lozano J, Saint F, Cordon-Cardo C. Defining molecular profiles of poor outcome in patients with invasive bladder cancer using oligonucleotide microarrays. J Clin Oncol. 2006; 24:778–789. [PubMed: 16432078]

Sanchez-Carbayo M, Socci ND, Lozano JJ, Li W, Charytonowicz E, Belbin TJ, et al. Gene discovery in bladder cancer progression using cDNA microarrays. Am J Pathol. 2003; 163:505–516. [PubMed: 12875971]

Smith SC, Oxford G, Baras AS, Owens C, Havaleshko D, Brautigan DL, et al. Expression of ral GTPases, their effectors, and activators in human bladder cancer. Clin Cancer Res. 2007; 13:3803–3813. [PubMed: 17606711]

Smith SC, Oxford G, Wu Z, Nitz MD, Conaway M, Frierson HF, et al. The metastasis-associated gene CD24 is regulated by Ral GTPase and is a mediator of cell proliferation and survival in human cancer. Cancer Res. 2006; 66:1917–1922. [PubMed: 16488989]

Stein JP, Lieskovsky G, Cote R, Groshen S, Feng AC, Boyd S, et al. Radical cystectomy in the treatment of invasive bladder cancer: long-term results in 1,054 patients. J Clin Oncol. 2001; 19:666–675. [PubMed: 11157016]

Su AI, Welsh JB, Sapinoso LM, Kern SG, Dimitrov P, Lapp H, et al. Molecular classification of human carcinomas by use of gene expression signatures. Cancer Res. 2001; 61:7388–7393. [PubMed: 11606367]

Team RDC. R Reference Manual. Network Theory; Vienna: 2003. p. 736pp

Theodorescu D, Sapinoso LM, Conaway MR, Oxford G, Hampton GM, Frierson HF Jr. Reduced expression of metastasis suppressor RhoGDI2 is associated with decreased survival for patients with bladder cancer. Clin Cancer Res. 2004; 10:3800–3806. [PubMed: 15173088]

Thykjaer T, Workman C, Kruhoffer M, Demtroder K, Wolf H, Andersen LD, et al. Identification of gene expression patterns in superficial and invasive human bladder cancer. Cancer Res. 2001; 61:2492–2499. [PubMed: 11289120]

Titus B, Frierson HF Jr, Conaway M, Ching K, Guise T, Chirgwin J, et al. Endothelin axis is a target of the lung metastasis suppressor gene RhoGDI2. Cancer Res. 2005; 65:7320–7327. [PubMed: 16103083]

van Delft JH, van Agen E, van Breda SG, Herwijnen MH, Staal YC, Kleinjans JC. Comparison of supervised clustering methods to discriminate genotoxic from non-genotoxic carcinogens by gene expression profiling. Mutat Res. 2005; 575:17–33. [PubMed: 15924884]

Witjes JA. Management of BCG failures in superficial bladder cancer: a review. Eur Urol. 2006; 49:790–797. [PubMed: 16464532]

Xu J, Moatamed F, Caldwell JS, Walker JR, Kraiem Z, Taki K, et al. Enhanced expression of nicotinamide N-methyltransferase in human papillary thyroid carcinoma cells. J Clin Endocrinol Metab. 2003; 88:4990–4996. [PubMed: 14557485]

Yao M, Tabuchi H, Nagashima Y, Baba M, Nakaigawa N, Ishiguro H, et al. Gene expression analysis of renal carcinoma: adipose differentiation-related protein as a potential diagnostic and prognostic biomarker for clear-cell renal carcinoma. J Pathol. 2005; 205:377–387. [PubMed: 15682440]

Zheng PS, Wen J, Ang LC, Sheng W, Viloria-Petit A, Wang Y, et al. Versican/PG-M G3 domain promotes tumor growth and angiogenesis. Faseb J. 2004; 18:754–756. [PubMed: 14766798]

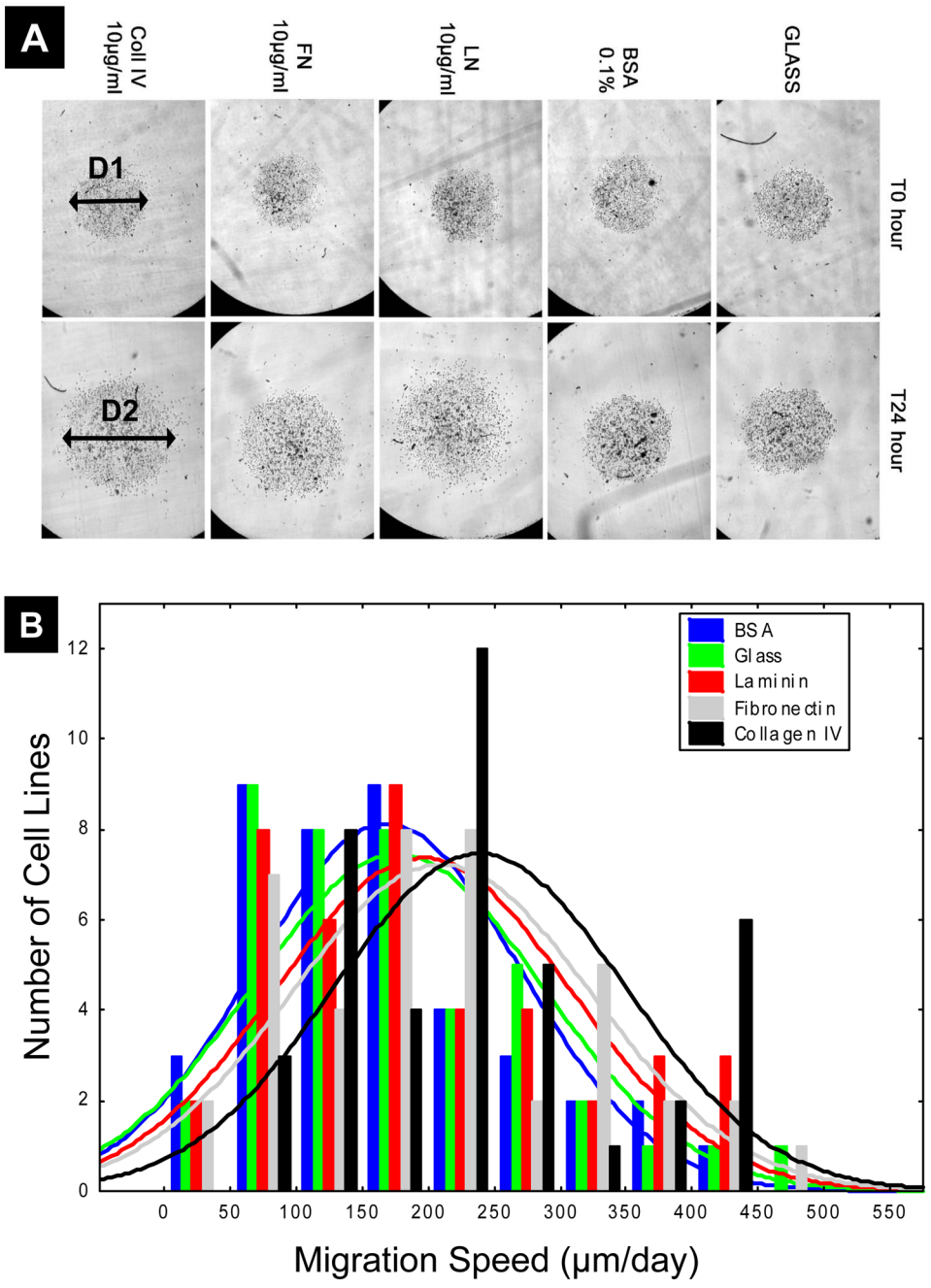

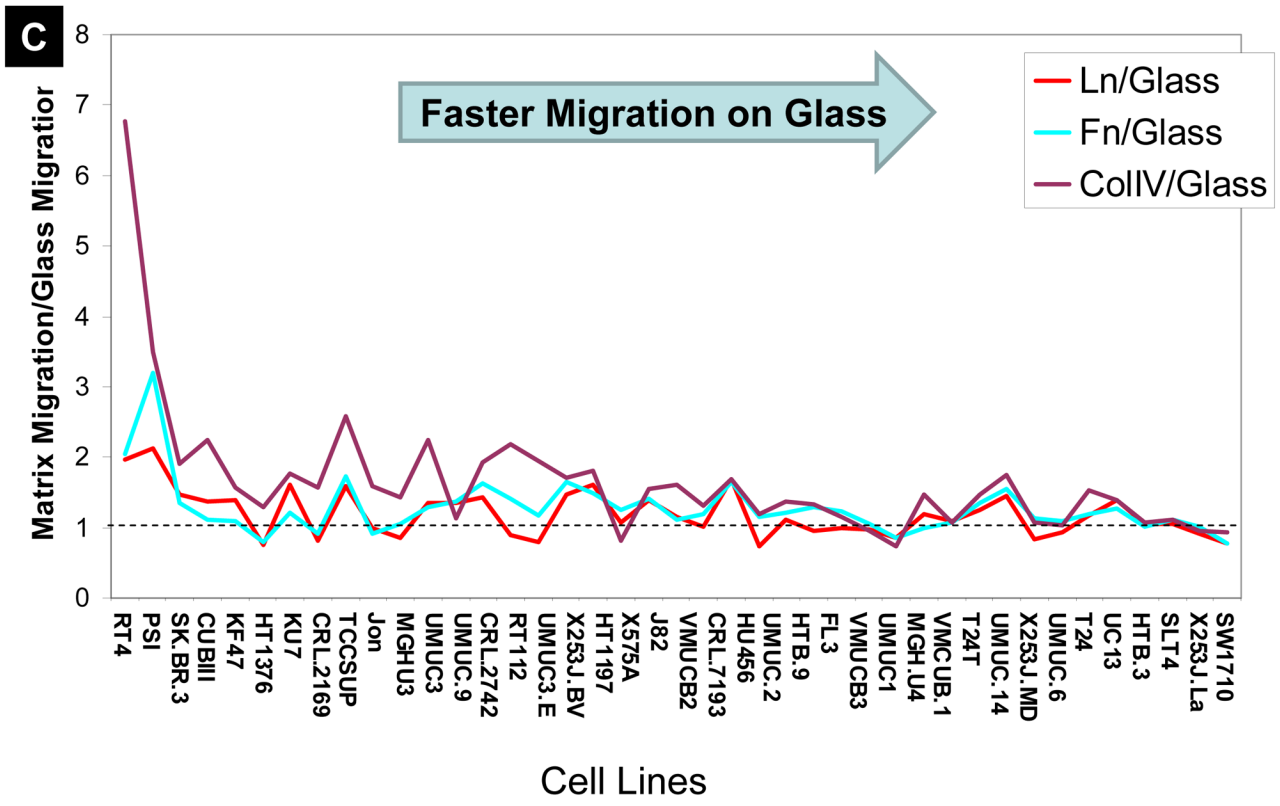

Figure 1. Cell Migration of human bladder cancer cell lines in Radial Migration Assay (RMA)

(A) Radial migration assay of UMUC3 (Oxford *et al.*, 2005) human bladder cancer cell lines on different matrices with phase contrast microscopy. **(B)** Histogram (with line smoothing) of migration speed distribution as a function of cell matrix substrate (Laminin (Ln) 10μg/ml, Collagen Type IV (Col lV) 10μg/ml, Fibronectin (Fn) 10μg/ml, BSA 0.1%, Glass) calculated from radial migration assay. **(C)** Ratio of migration speed on matrices to that of migration speed on glass, rank ordered as a function of migration on glass shown in Table 1.

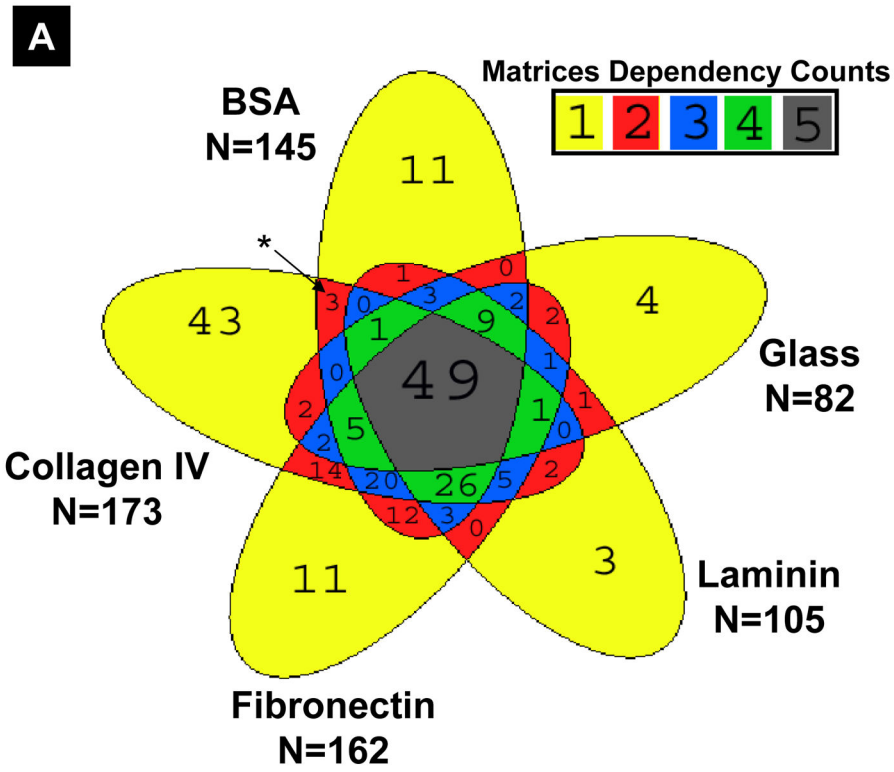

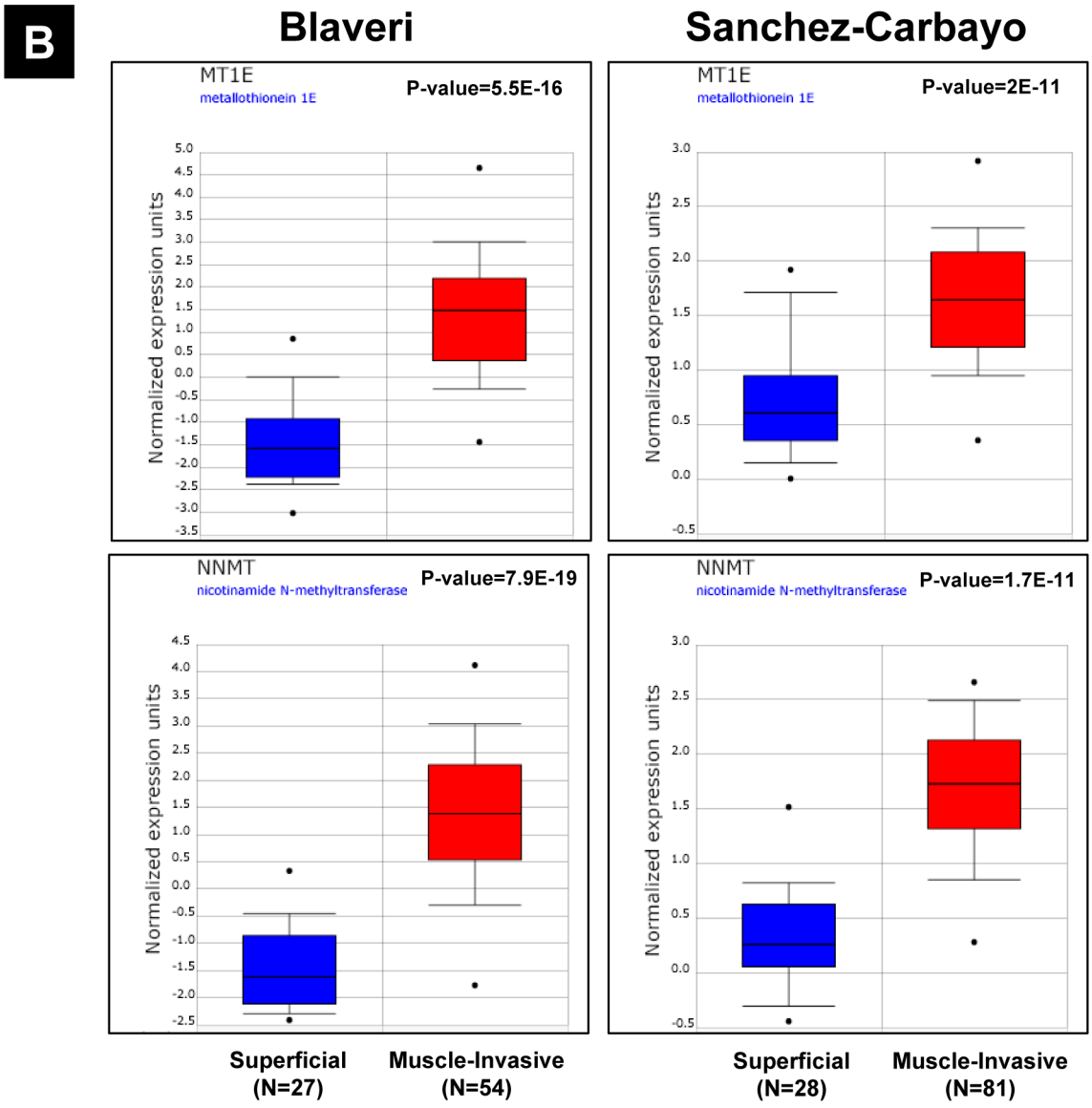

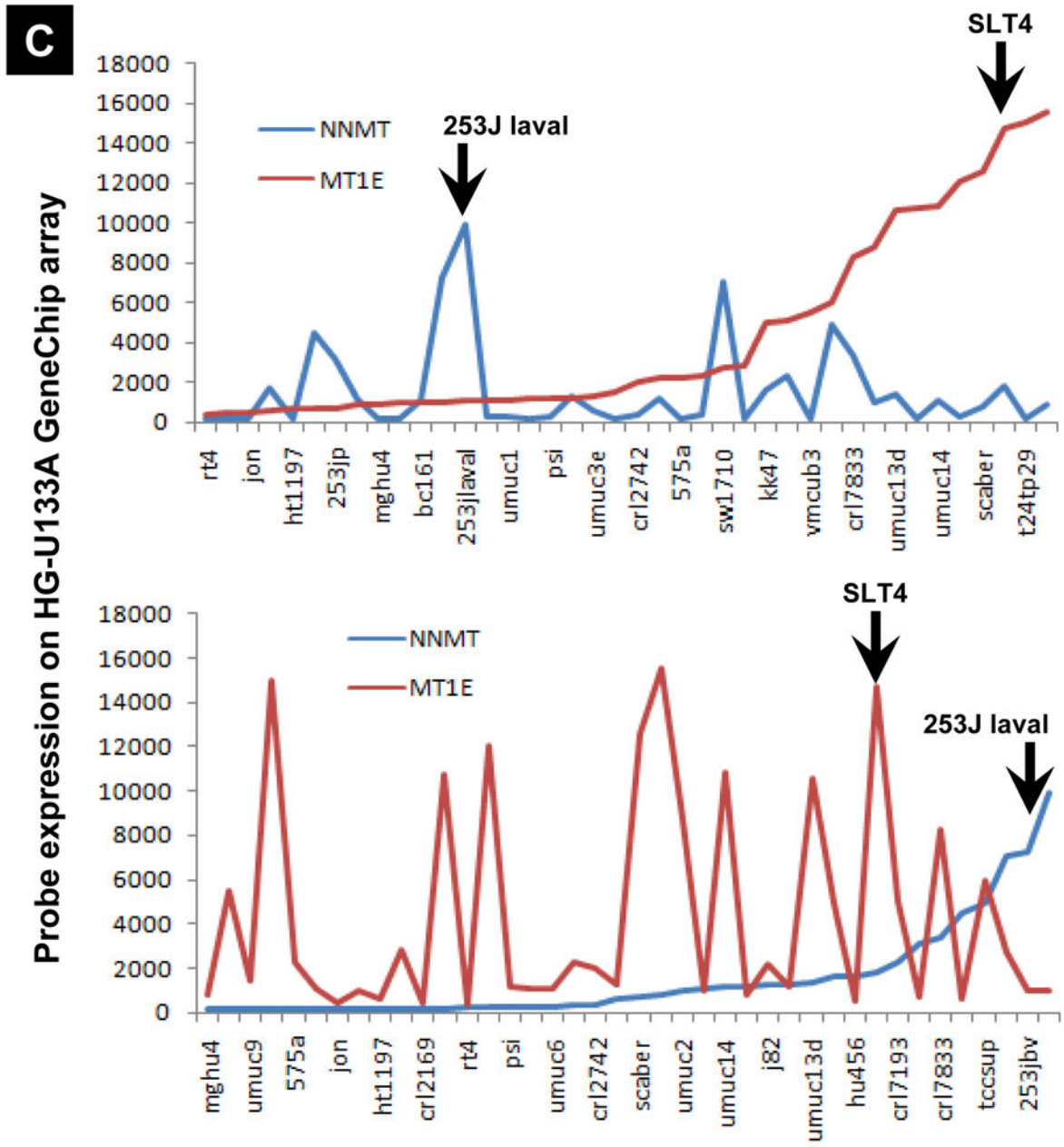

Figure 2.

(A) Distribution of the numbers of gene probes associated with cell migration as a function of cell matrix substrate The number on each region represents the number of gene probes dependent on one or more matrix type. Dependency is defined in materials and methods. The color of the area indicates the number of matrix types the specified gene probes are associated with. * For example, 3 probes are associated with a dependency on BSA and collagen IV. **(B)** The relationship of NNMT and MT1E expression to tumor stage in two independent studies of human bladder cancer (Blaveri *et al.*, 2005; Sanchez-Carbayo *et al.*, 2006). Data and statistics obtained from www.oncomine.org. **(C)** NNMT and MT1E probe expression in the 40 human bladder cancer cell lines on HG-U133A GeneChip array

(Affymetrix). The cells used for functional studies 253J laval and SLT4 are shown. X axis shows selected cell line names. All cell line names are avalable in Figure 1D.

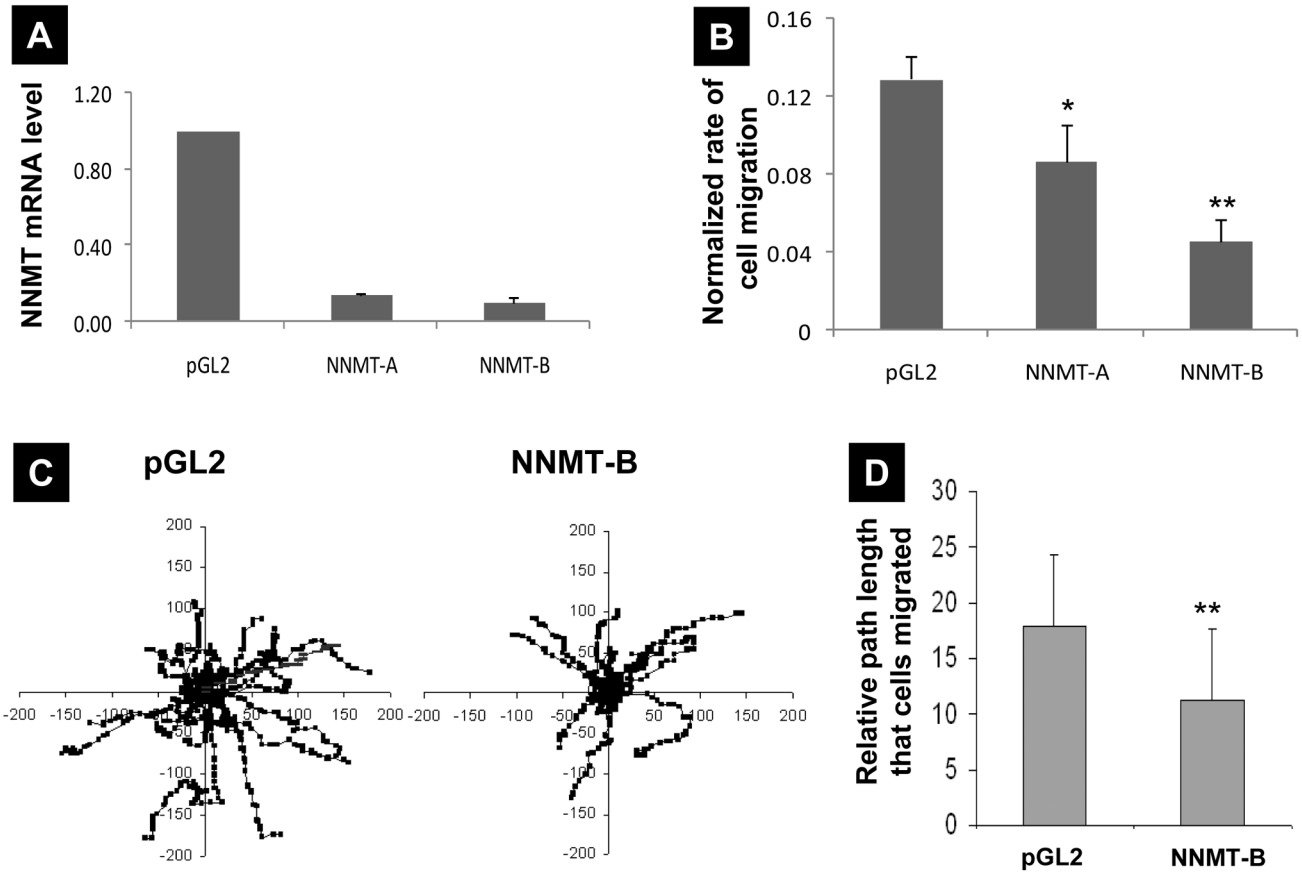

Figure 3. Effect of NNMT depletion on 253J laval human bladder cancer cell migration

(A) Real-time PCR for NNMT mRNA. The NNMT expression is reduced to 14 ± 1 % for NNMT-A siRNA knockdown and 10 ± 3 % for NNMT-B siRNA knockdown. Error bars are standard deviation from the mean. **(B)** Cells were transfected with either of two NNMT-specific siRNA oligonucleotides or luciferase pGL2, and evaluated after 6 h in a Boyden chamber using 2% FBS as the chemoattractant. NNMT-A and NNMT-B siRNA oligonucleotide caused decreased chemotaxis of 253 J laval by 23% (*p=0.037) and 64% (**p<0.001), respectively relative to pGL2 control. The result was repeated four times with similar results. Error bars are standard deviation from the mean. **(C)** Time lapse microscope is used to track the monolayer movements of individual 253J cells over a time course of up to three hours for 27 NNMT-knockdown and 21 luciferase-knockdown individual cells. **(D)** The average path length that cells traveled in C was quantified and shown (*p<0.001). Error bars are standard deviation from the mean. No effects on cell number were noted during the time course (3 and 6 hrs) of the migration assay (Figure 5).

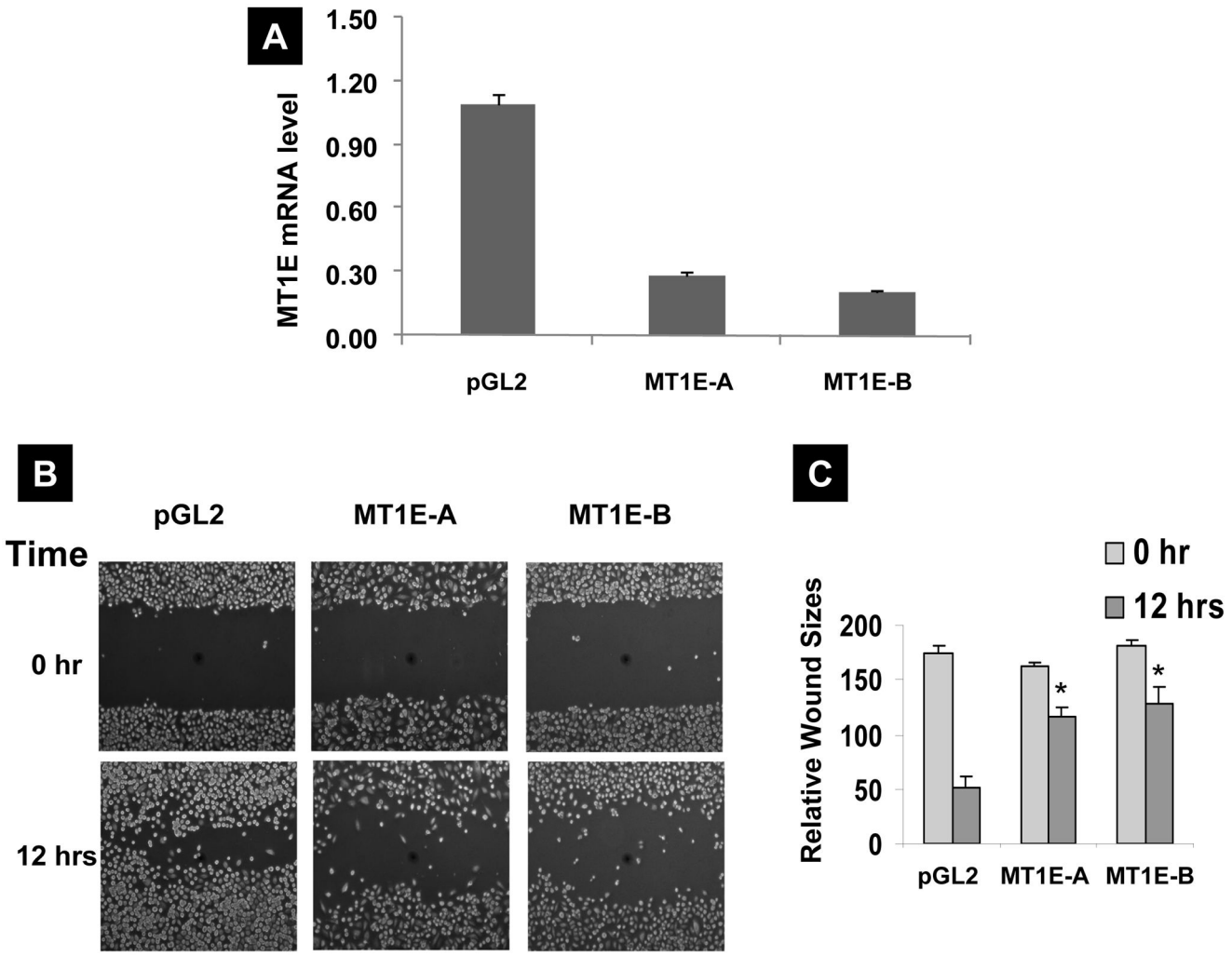

Figure 4. Wound healing of SLT4 human bladder cancer cells after knockdown of MT1E

MT1E depletion inhibits wound healing. 1×10^5 of SLT4 cells were transfected with the indicated siRNA, wounded 48 hours post transfection, and healing was followed for 12 hours. The panels shown are the result in one representative experiment of three. **(A)** Real-time PCR of MT1E mRNA expression. The MT1E expression is reduced to 25.5 ± 2 % for MT1E-A siRNA knockdown and 19.3 ± 1 % for MT1E-B siRNA knockdown, compared to its control. **(B)** Phase contrast micrographs (100X) of cells immediately after and at 12 hours after wounding. **(C)** Plotting of scratch wound assay; bar and error bar indicates the mean and standard deviation respectively of values obtained from triplicate samples in three separate experimental sets (*p<0.001 for comparison to pGL2 wound at 12 hrs). No effects on cell number were noted during the time course (12 hrs) of the migration assay (Figure 5).

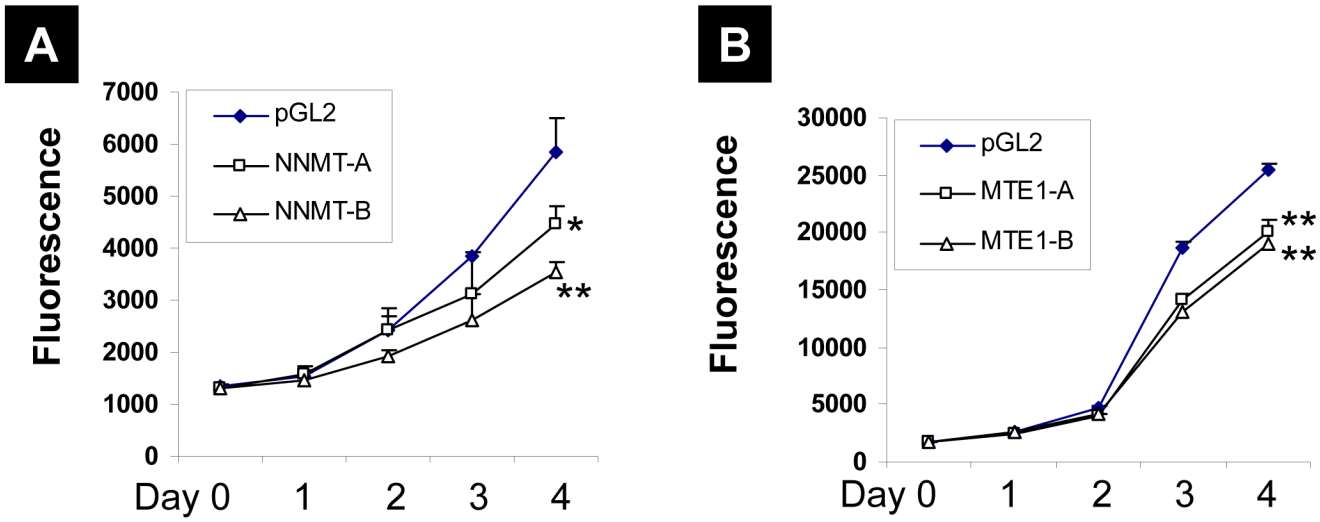

Figure 5. Cell proliferation following MT1E or NNMT gene depletion

Cells (5×10^3/well) transfected with pGL2, NNMT-A or NNMT-B siRNA were inoculated in 24 well plates. At the designated time point post seeding, cell numbers were estimated by using Alamar Blue assay. **(A)** Growth curves in 253J laval cells following knockdown of NNMT (*p=0.048, **p=0.019). **(B)** Growth curves in SLT4 cells following knockdown of MT1E (**p=0.003). Point and error bar indicates the mean and standard deviation respectively of values obtained from triplicate samples in three separate experimental sets.

Table 1

Radial Migration Assay speed of human bladder cancer cell lines on different matrices

Cell line	Glass^ Mean±Stdev	BSA Mean±Stdev	Fn Mean±Stdev	Ln Mean±Stdev	ColIV Mean±Stdev
SW1710	461.33±103.71*	391.87±76.24*	358.37±81.61*	354.95±39.88*	429.02±93.87*
X253J.La	446.93±87.82*	437.81±95.7*	456.9±90.22*	411.95±63.23*	422.41±60.15*
SLT4	395.66±51.59*	328.26±48.87*	439.86±62*	413.59±49.57*	437.4±48.73*
HTB.3	342.16±62.07*	352.01±41.17*	349.75±41.07*	359.81±34.86*	367.2±73.48*
UC13	321.42±51.61*	328.59±53.15*	407.4±58.35*	445.57±63.14*	445.11±40.37*
T24	282.05±60.25*	266.14±75.72*	336.36±65.98*	329.17±63.07*	432.82±96.15*
UMUC.6	276.07±61.1*	285.51±31.09*	301.31±46.14*	258±39.19*	285.71±68.25*
X253J.MD	264.33±25.11*	230.89±34.79*	300.93±35.96*	219.75±41.83	283.62±52.25*
UMUC.14	255.06±37.82*	251.23±37.89*	394.83±68.42*	367.24±55.52*	445.54±27.71*
T24T	252.71±55.65*	237.78±45.19*	342.16±62.16*	316.3±61.83*	371.1±92.84*
VMCUB.1	247.87±83.35*	249.38±108.63*	263.34±112.87*	269.82±82.19*	267.04±130.96
MGH.U4	226.01±64.77*	176.17±64.95	222.76±95.56	269.99±78.86*	330.77±69.18*
UMUC1	220.24±54.05*	197.04±85.9	190.07±84.72	188.42±58.4	160.92±75.24*
VMUCB3	216.95±57.4*	163.59±44.68	226.19±61.38	211.62±38.71	208.33±27.48
FL3	199.87±58.37	164.33±85.13	244.65±60.54*	199.46±45.17	231.16±53.62
HTB.9	180.25±95.55	206±129.32	233.37±79.99	170.16±89.87	241.17±86
total mean	**174.36±174.36**	**168.58±115.87**	**209.71±127.34**	**194.98±123.81**	**237.89±124.67**
UMUC.2	167.08±95.41	102.01±59.6*	193.56±24.19	122.95±76.28*	198.16±36.54*
HU456	166.14±75.64	169.4±40.02	275.25±56.98*	280.17±54.16*	281.81±42.03*
CRL.7193	160.34±44.54	128.75±44.43	189.41±42.81	161.89±53.32	210.27±34.71
VMUCB2	159.07±119.53	144.5±111.54	176.31±111.73	181.86±113.22	256.57±129.9
J82	150.04±27.86	146.44±32.92	212.49±20.34	207.39±22.36	233.8±28.59
X575A	149.8±66.4	122.51±77.03	187.75±83.55	160.9±49.16	122.95±101.98*

Cell line	Glass^ Mean±Stdev	BSA Mean±Stdev	Fn Mean±Stdev	Ln Mean±Stdev	ColIV Mean±Stdev
HT1197	135.88±95.92*	169.75±65.93	201.35±88.33	217.78±59.16	244.46±44.09
X253J.BV	129.93±59.06*	168.51±27.38	214.08±35.62	191.5±51.37	221.06±34.74
UMUC3.E	115.86±38.56*	94.29±50.56*	135.99±24.67*	92.64±31.92*	226.16±69.16
RT112	110.84±70.66*	103.45±63.16*	156.2±50.67*	98.3±74.88*	241.13±74.96
CRL.2742	109.61±49.33*	157.22±30.2	177.75±49.2	156.2±59.4*	210.18±56.96
UMUC.9	108.99±39.24*	71.2±70.6*	148.23±68.96*	146.31±71.78*	123.65±84.1*
UMUC3	103.08±34.81*	133.88±35.26	133.06±51.01*	139.43±59.84*	231.17±80.24
MGHU3	94.01±42.62*	106.53±38.95*	98.11±27.34*	80.67±33.82*	133.47±44.67*
Jon	78.59±18.71*	69.86±35.15*	72.04±31.86*	78.19±56.96*	124.99±32.59*
TCCSUP	71.19±37.69*	71.63±22.34*	122.74±35.63*	112.48±30.98*	183.09±32.1*
CRL.2169	67.17±20.52*	66.5±35.15*	60.68±32.72*	54.39±46.37*	105.71±52.58*
KU7	64.24±24.53*	70.38±36.59*	77.59±50.76*	102.83±28.76*	113.1±40.19*
HT1376	60.76±23.89*	44.54±22.56*	47.82±19.18*	45.36±36.39*	78±15.05*
KF47	58.29±27.24*	42.69±21*	63.63±34.88*	80.46±25.53*	91.95±16.9*
CUBIII	54.41±32.87*	57.77±39.23*	60.34±34.82*	74.79±42.49*	122.13±32.34*
SK.BR.3	50.08±20.83*	78.37±41.59*	67.73±18.33*	73.89±37.4*	95.24±21.91*
PSI	49.06±51.18*	62.25±41.49*	156.75±45.35*	104.68±33.05*	171.08±41.49*
RT4	18.06±48.19*	48.81±68.8*	36.95±51.31*	35.51±73.36*	122.13±33.05*

^ Rank ordered

* $p<0.05$ compared to mean (see Materials and Methods). Indicates Rapid (if above total mean) or Slow (if below total mean) cell lines in each matrix group.

Abbreviations: BSA: Bovine serum albumin; Fn: Fibronectin; Ln: Laminin; ColIV: Type 4 collagen

Matrix concentrations are provided in Materials and Methods

** As defined in Materials and Methods

Table 2

Pathways involved in cell migration on different surfaces and matrices

Surface or matrix	Migration Rate ^ Mean (SD dev)	Ecosanoid	Wnt/β-Catenin	Integrin	O-Glycan Biosynthesis
Glass (4 *)	174.36 (123.04)		−1.8 **	−1.6	
BSA (11)	168.58 (115.87)	−3.8	−1.7	−1.4	
Laminin (3)	194.98 (123.81)	−2.8		−1.7	
Fibronectin (11)	209.71 (127.34)	−3.5	−1.6		
Collagen IV (43)	237.89 (124.67)	−2.2		−2.2	−2.7
All Surfaces (49)					−1.4

* Probes associated with migration rate only on specified surface (from Figure 2A)

** Log significance from Ingenuity output (www.ingenuity.com)

^ Of entire set of bladder cancer cell lines (from Table 1)

Oncogene. Author manuscript; available in PMC 2017 March 30.

Table 3

Gene expression differences found with the analysis of cell migration in vitro compared to normal bladder and tumor stage of primary human bladder tumors

Probes	Probe description	glass	BSA	Ln	Fn	ColIV	Normal^ (N=15)	Ta^ (N=25)	T2–4^ (N=21)
Matrix Dependent Probes (laminin, fibronectin and collagen IV)									
221731_x_at	chondroitin sulfate proteoglycan 2 (versican)	0#	0	1#	1	1	158*	330	807
204620_s_at	chondroitin sulfate proteoglycan 2 (versican)	0	0	1	1	1	234	448	1061
202237_at	nicotinamide N-methyltransferase (NNMT)	0	0	0	1	1	187	129	453
209173_at	putative secreted protein XAG mRNA	0	0	0	1	1	863	1076	630
202668_at	ephrin-B2	0	0	0	1	1	118	186	401
202016_at	mesoderm specific transcript (mouse) homolog (MEST)	0	0	0	1	1	86	288	401
202628_s_at	plasminogen activator inhibitor type 1	0	0	1	0	0	133	84	228
210495_x_at	fibronectin 1	0	0	0	1	0	1299	903	2908
204470_at	GRO1 oncogene (melanoma growth stimulating activity, alpha)	0	0	0	1	0	66	69	132
201842_s_at	EGF-containing fibulin-like extracellular matrix protein 1	0	0	0	0	1	210	234	234
205157_s_at	keratin 17 (KRT17)	0	0	0	0	1	406	538	1871
209386_at	transmembrane 4 superfamily member 1	0	0	0	0	1	323	181	501
212992_at	CLONE=IMAGE:2464769	0	0	0	0	1	66	54	217
209699_x_at	dihydrodiol dehydrogenase mRNA	0	0	0	0	1	1668	2566	1226
204151_x_at	aldo-keto reductase family 1, member C1 (AKR1C1)	0	0	0	0	1	1983	3067	1399
216594_x_at	chlordecone reductase homolog (clone HAKRc)	0	0	0	0	1	1554	2562	1115
200600_at	moesin (MSN)	0	0	0	0	1	173	169	258
217762_s_at	RAB31, member RAS oncogene family	0	0	0	0	1	219	212	468
201130_s_at	E-cadherin	0	0	0	0	1	53	134	76
206595_at	cystatin EM (CST6)	0	0	0	0	1	34	43	178
Matrix Independent Probes (BSA and glass)									
212859_x_at	metallothionein 1E (MT1E)	1	1	0	0	0	863	1076	1630
212464_s_at	fibronectin 1	1	0	0	0	0	1100	788	2865
208791_at	clusterin (testosterone-repressed prostate message 2)	1	0	0	0	0	848	457	292

Probes	Probe description	glass	BSA	Ln	Fn	ColIV	Normal^ (N=15)	Ta^ (N=25)	T2–4^ (N=21)
202609_at	epidermal growth factor receptor pathway substrate 8 (EPS8)	0	1	0	0	0	324	568	319

#Significant (1) or non significant status (0) based on p value for the LPE test for testing the null hypothesis of equal mean gene expression across in both slow and fast migratory cells

^Normal, Ta and T2–4 represent normal urothelium and tumor stages

N indicates the number of samples in each group

*Expression level of probe